Supporting Information

Guerbet Glycolipids from Mannose: Liquid Crystals Properties

Melonney Patrick[a], N. Idayu Zahid[a], Manfred Kriechbaum[b], and Rauzah Hashim[a]

[a] Centre for Fundamental and Frontier Sciences in Nanostructure Self-Assembly, Department of Chemistry, Faculty of Science, University of Malaya, 50603, Kuala Lumpur, Malaysia.

[b] Institute of Inorganic Chemistry, Graz University of Technology, Stremayrgasse 9, 8010 Graz, Austria

Table of Contents

^{1}H NMR and ^{13}C NMR for the synthetic Guerbet mannosides

2-ethyl-hexyl-*α*-D-mannopyranoside, *α*-Man-OC$_6$C$_2$

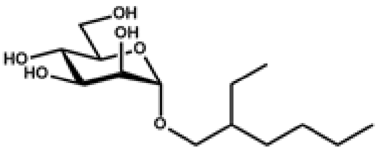

^{1}H NMR (400 MHz, CD_3OD): δ (ppm) = 0.90–0.94 (t, 6H, J = 6.8 Hz, 2 x CH_3), 1.32–1.50 (m, 8H, CH_2), 1.52 (m, 1H, CH), 3.33 (m, 2H, OCH_2), 3.54 (ddd, 1H, $J_{5,6a}$ = 2.4 Hz, H-5), 3.64 (t, 1H, $J_{4,5}$ =9.2 Hz, H-4), 3.68-3.76 (m, 1H, $J_{5,6b}$ = 5.6 Hz, H-6b), 3.68-3.76 (m, 1H, $J_{3,4}$ = 9.2 Hz, H-3), 3.80 (dd, 1H, $J_{2,3}$ = 3.2 Hz, H-2), 3.83 (dd, 1H, $J_{6a,6b}$ = 11.6 Hz, H-6a), 4.73 (d, 1H, $J_{1,2}$ = 1.6 Hz, H-1)

^{13}C NMR (400 MHz, CD_3OD): δ (ppm) = 100.4 (C-1), 73.3 (C-5), 71.3 (C-3), 70.9 (C-2), 69.8 (C-4), 67.2 (OCH_2), 61.5 (C-6), 39.6 (CH), 22.7–30.4 (CH_2), 13.0, 10.1 (CH_3)

2-butyl-octyl-*α*-D-mannopyranoside, *α*-Man-OC$_8$C$_4$

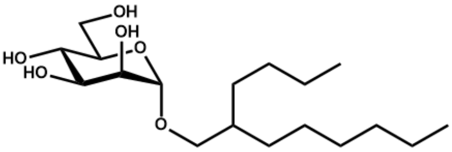

^{1}H NMR (400 MHz, CD_3OD): δ (ppm) = 0.90–0.94 (t, 6H, J = 6.8 Hz, 2 x CH_3), 1.32–1.50 (m, 16H, CH_2), 1.58 (m, 1H, CH), 3.33 (m, 2H, OCH_2), 3.54 (ddd, 1H, $J_{5,6a}$ = 2.4 Hz, H-5), 3.64 (t, 1H, $J_{4,5}$ =9.2 Hz, H-4), 3.68-3.76 (m, 1H, $J_{5,6b}$ = 5.6 Hz, H-6b), 3.68-3.76 (m, 1H, $J_{3,4}$ = 9.2 Hz, H-3), 3.80 (dd, 1H, $J_{2,3}$ = 3.0 Hz, H-2), 3.83 (dd, 1H, $J_{6a,6b}$ = 11.6 Hz, H-6a), 4.72 (d, 1H, $J_{1,2}$ = 1.2 Hz, H-1)

^{13}C NMR (400 MHz, CD_3OD): δ (ppm) = 100.4 (C-1), 73.3 (C-5), 71.4 (C-3), 70.9 (C-2), 70.2 (C-4), 67.1 (OCH_2), 61.5 (C-6), 37.9 (CH), 22.3–31.6 (CH_2), 13.0 (CH_3)

2-hexyl-decyl-*α*-D-mannopyranoside, *α*-Man-OC$_{10}$C$_6$

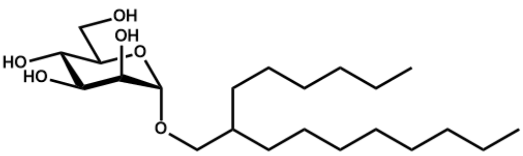

^{1}H NMR (400 MHz, CD_3OD): δ (ppm) = 0.90–0.94 (t, 6H, J = 6.4 Hz, 2 x CH_3), 1.32–1.50 (m, 24H, CH_2), 1.59 (m, 1H, CH), 3.33 (m, 2H, OCH_2), 3.54 (ddd, 1H, $J_{5,6a}$ = 2.4 Hz, H-5), 3.64 (t, 1H, $J_{4,5}$ =9.2 Hz, H-4), 3.67-3.76 (m, 1H, $J_{5,6b}$ = 5.6 Hz, H-6b), 3.67-3.76 (m, 1H, $J_{3,4}$ = 9.2 Hz, H-3), 3.80 (dd, 1H, $J_{2,3}$ = 3.2 Hz, H-2), 3.83 (dd, 1H, $J_{6a,6b}$ = 11.6 Hz, H-6a), 4.72 (d, 1H, $J_{1,2}$ = 1.6 Hz, H-1)

^{13}C NMR (400 MHz, CD_3OD): δ (ppm) = 100.5 (C-1), 73.2 (C-5), 71.4 (C-3), 70.9 (C-2), 70.2 (C-4), 67.1 (OCH_2), 61.5 (C-6), 37.9 (CH), 22.3–31.7 (CH_2), 13.0 (CH_3)

2-octyl-dodecyl-*α*-D-mannopyranoside, *α*-Man-OC$_{12}$C$_8$

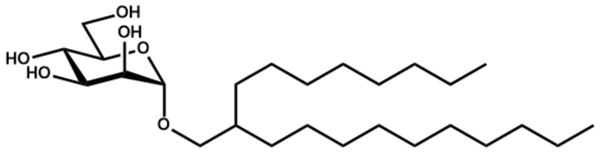

^{1}H NMR (400 MHz, CD_3OD): δ (ppm) = 0.90–0.94 (t, 6H, J = 6.4 Hz, 2 x CH_3), 1.32–1.50 (m, 32H, CH_2), 1.59 (m, 1H, CH), 3.33 (m, 2H, OCH_2), 3.54 (ddd, 1H, $J_{5,6a}$ = 2.4 Hz, H-5), 3.65 (t, 1H, $J_{4,5}$ =9.6 Hz, H-4), 3.67-3.76 (m, 1H, $J_{5,6b}$ = 5.6 Hz, H-6b), 3.67-3.76 (m, 1H, $J_{3,4}$ = 9.2 Hz, H-3), 3.80 (dd, 1H, $J_{2,3}$ = 3.2 Hz, H-2), 3.83 (dd, 1H, $J_{6a,6b}$ = 11.6 Hz, H-6a), 4.72 (d, 1H, $J_{1,2}$ = 1.6 Hz, H-1)

^{13}C NMR (400 MHz, CD_3OD): δ (ppm) = 100.5 (C-1), 73.2 (C-5), 71.4 (C-3), 70.9 (C-2), 70.2 (C-4), 67.1 (OCH_2), 61.5 (C-6), 37.9 (CH), 22.3–31.7 (CH_2), 13.0 (CH_3)

2-decyl-tetradecyl-*α*-D-mannopyranoside, *α*-Man-OC$_{14}$C$_{10}$

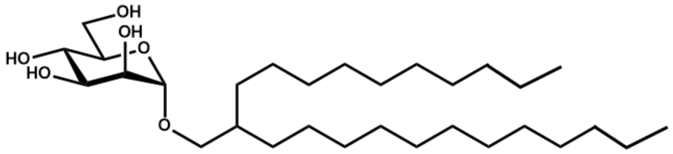

^{1}H NMR (400 MHz, CD_3OD): δ (ppm) = 0.90–0.94 (t, 6H, J = 6.4 Hz, 2 x CH_3), 1.32–1.48 (m, 40H, CH_2), 1.59 (m, 1H, CH), 3.33 (m, 2H, OCH_2), 3.54 (ddd, 1H, $J_{5,6a}$ = 2.4 Hz, H-5), 3.65 (t, 1H, $J_{4,5}$ =9.2 Hz, H-4), 3.67-3.76 (m, 1H, $J_{5,6b}$ = 5.2 Hz, H-6b), 3.67-3.76 (m, 1H, $J_{3,4}$ = 9.6 Hz, H-3), 3.80 (dd, 1H, $J_{2,3}$ = 3.6 Hz, H-2), 3.83 (dd, 1H, $J_{6a,6b}$ = 11.6 Hz, H-6a), 4.72 (d, 1H, $J_{1,2}$ = 1.6 Hz, H-1)

^{13}C NMR (400 MHz, CD_3OD): δ (ppm) = 100.5 (C-1), 73.2 (C-5), 71.4 (C-3), 70.9 (C-2), 70.2 (C-4), 67.1 (OCH_2), 61.5 (C-6), 37.9 (CH), 22.4–31.7 (CH_2), 13.1 (CH_3)

Fourier Transform Infra Red (FTIR)

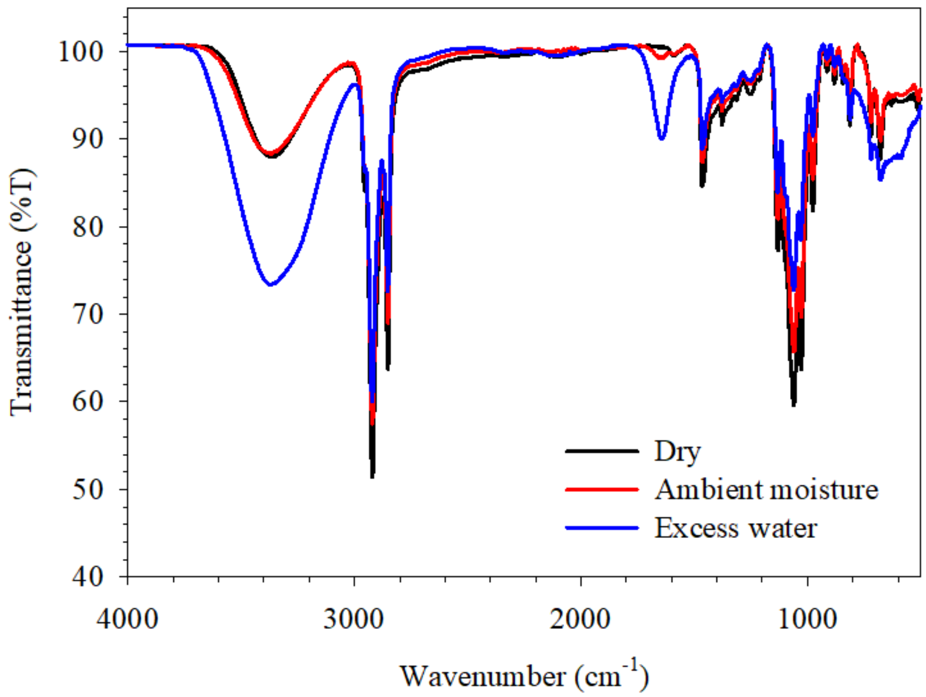

Figure S1. FTIR spectra for α-Man-OC$_{14}$C$_{10}$ at the room temperature in dry (after lyophilised in freeze dryer for at least 48 hours), left in ambient moisture for 96 hours and in excess water form.

Small- and Wide-Angle X-Ray Scattering (SWAXS)

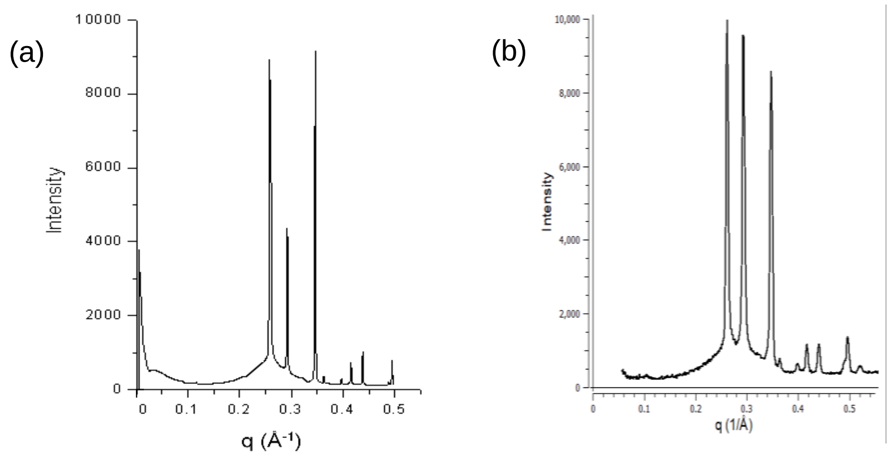

Figure S2. Small-angle X-ray scattering pattern for α-Man-OC$_{10}$C$_6$ obtained at (a) Australian Synchrotron; (b) Graz University of Technology. Both patterns measured with a point-shaped beam.

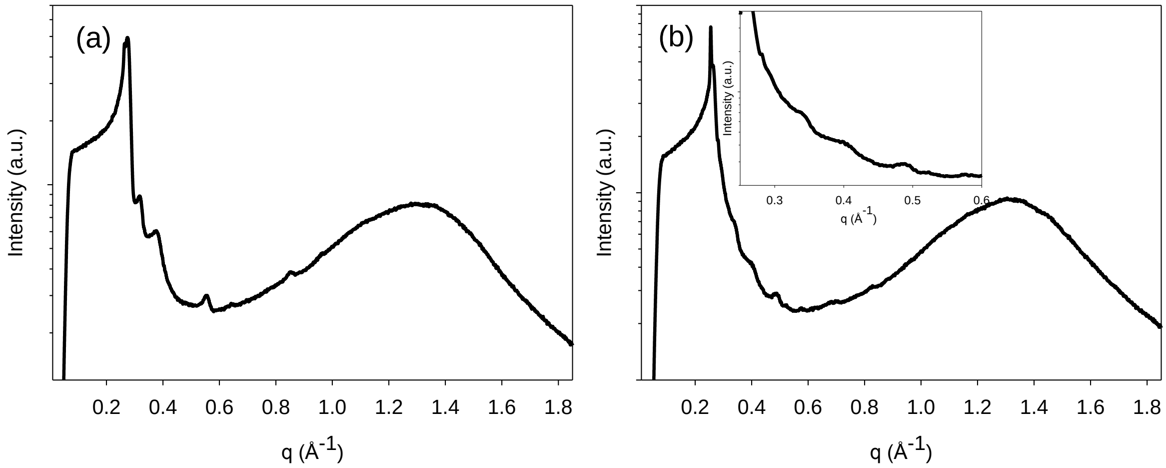

Figure S3. X-ray scattering pattern including wide-angle region for (a) *α*-Man-OC_8C_4 at 25°C and (b) *α*-Man-$OC_{10}C_6$ at 25°C.

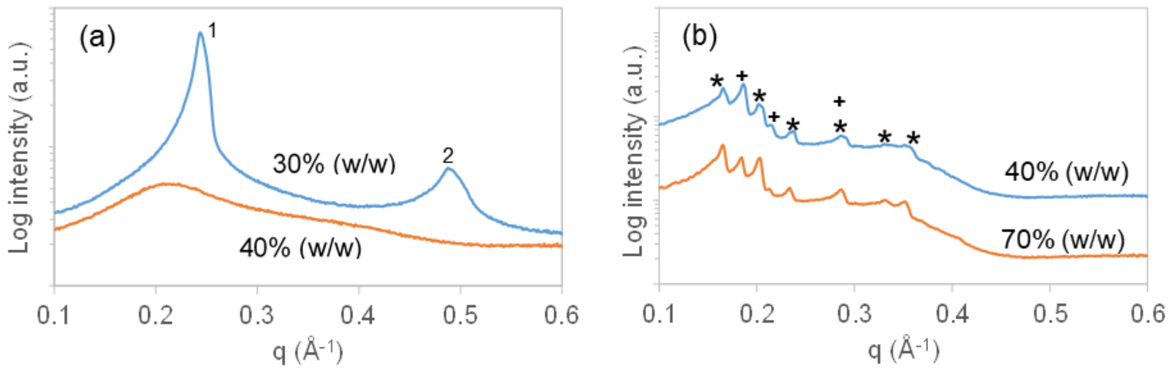

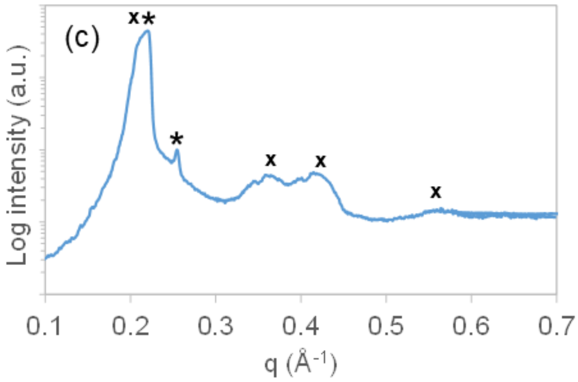

Figure S4. Small-angle X-ray scattering pattern at 25°C for (a) *α*-Man-OC_6C_2 at 30% (w/w) and 40% (w/w) showing an L_α and L_1 reflection respectively; (b) *α*-Man-$OC_{10}C_6$ at 40% (w/w) and 70% (w/w) displaying coexistence of *Ia*3*d* (denoted by the symbol (+) with reciprocal spacing ratios √6, √8, √14) and *Pn*3*m* (denoted by the symbol (*) with reciprocal spacing ratios √2, √3, √4, √6, √8, √9) phases and (c) *α*-Man-$OC_{12}C_8$ at 7.5% (w/w) portraying coexistence of *Pn*3*m* (denoted by the symbol (*) with reciprocal spacing ratios √2, √3) and H_2 phase denoted by the symbol (x) with reciprocal spacing ratios √1, √3, √4, √7. All phases were formed at excess water region except in (c).

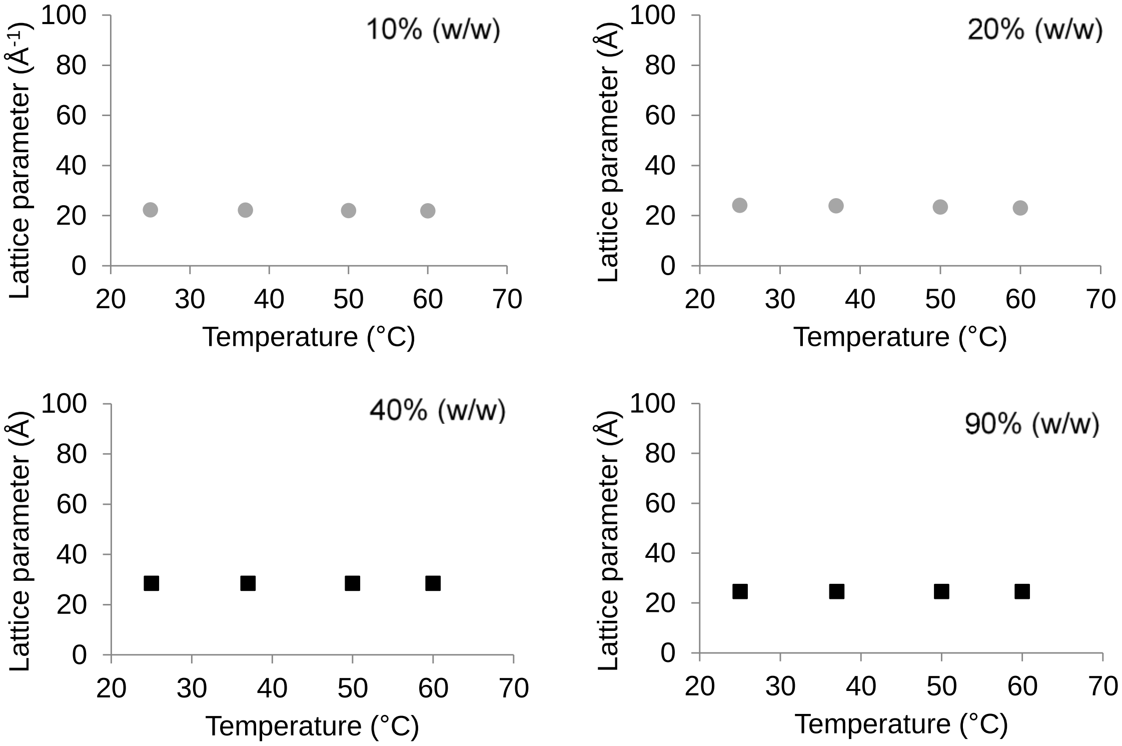

Figure S5. Temperature dependence of the lattice parameter for α-Man-OC_6C_2/water system. Symbols: ● (L_α) and ■ (L_1).

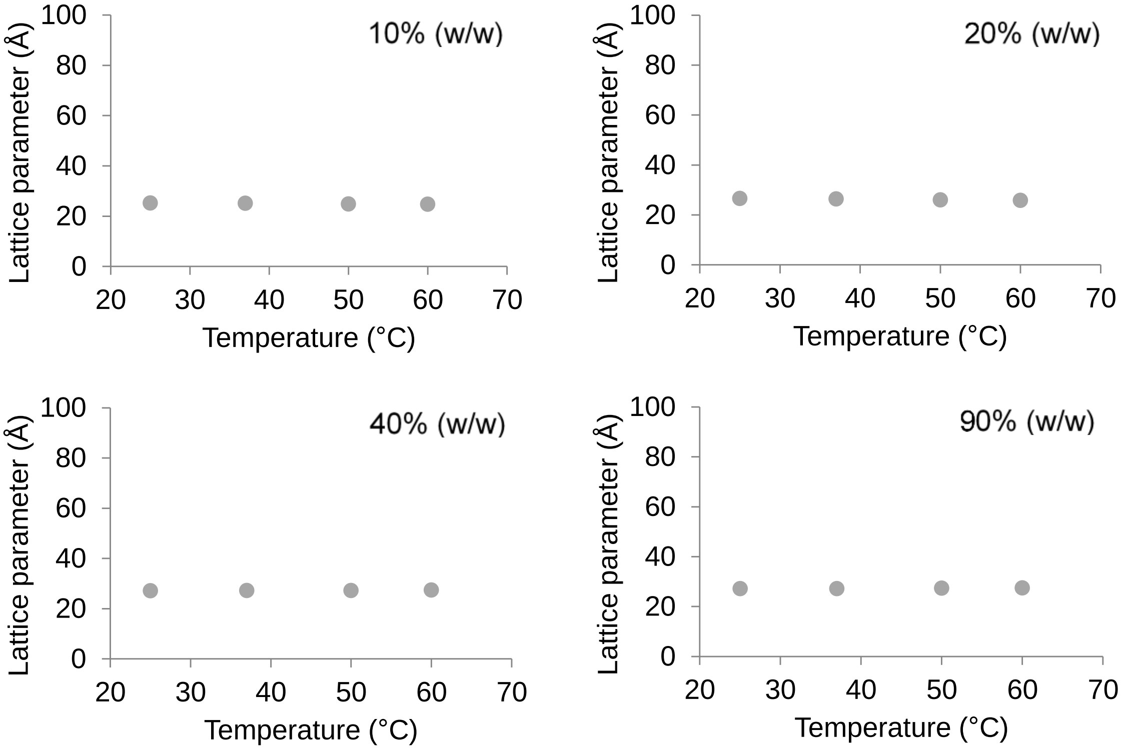

Figure S6. Temperature dependence of the lattice parameter for α-Man-OC_8C_4/water system. Symbols: ● (L_α).

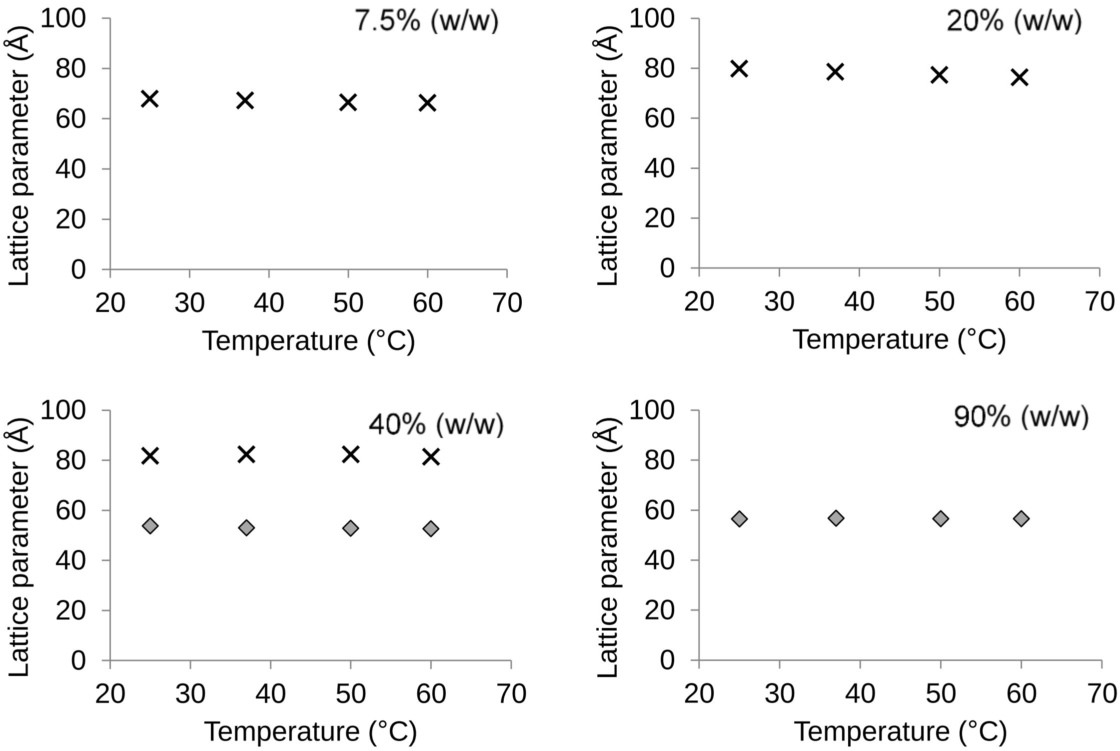

Figure S7. Temperature dependence of the lattice parameter for *α*-Man-$OC_{10}C_6$/water system. Symbols: ✕ (*Ia*3*d*) and ◆ (*Pn*3*m*).

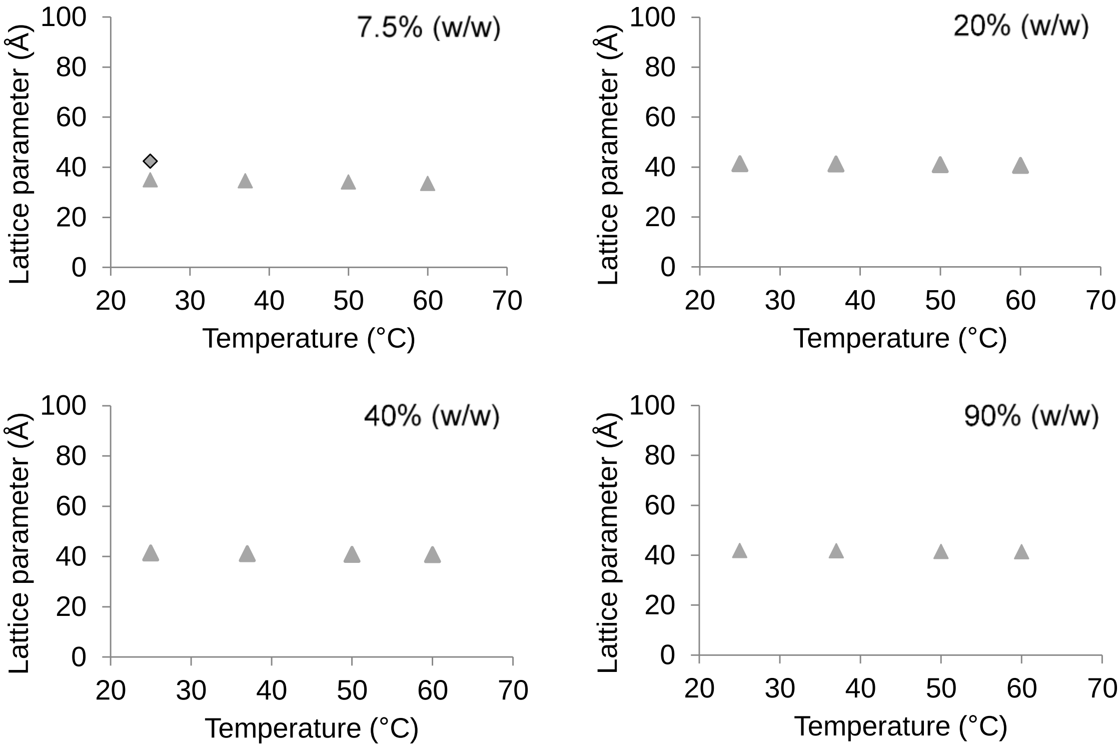

Figure S8. Temperature dependence of the lattice parameter for *α*-Man-$OC_{12}C_8$/water system. Symbols: ◆ (*Pn*3*m*) and ▲ (H_2).

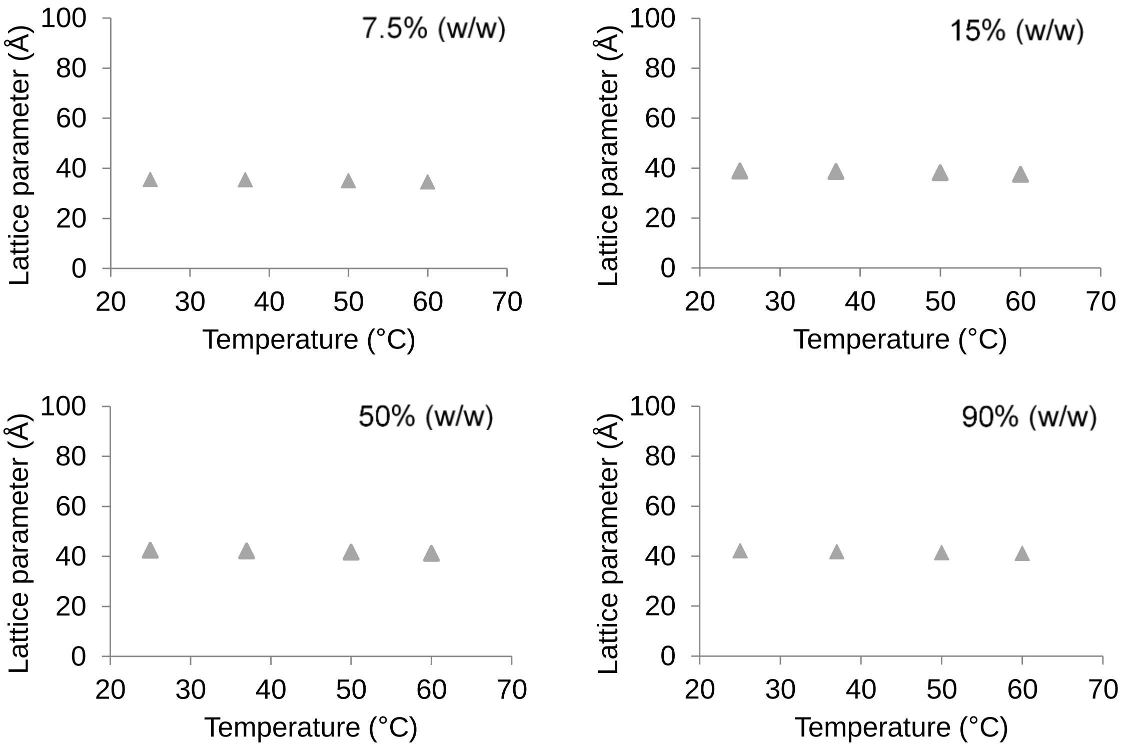

Figure S9. Temperature dependence of the lattice parameter for *α*-Man-$OC_{14}C_{10}$/water system. Symbols: ▲ (H_2).

Table S1. Lattice parameter of α-Man-OC_6C_2 as a function of water content and temperature.

Water Content (% (w/w))	Temperature (°C)	Lattice parameter (Å)	
		L_α	L_1
0	25	20.6	
0	37	20.6	
0	50	20.6	
0	60	20.6	
10	25	22.3	
10	37	22.2	
10	50	22.0	
10	60	21.9	
20	25	24.1	
20	37	23.9	
20	50	23.5	
20	60	23.1	
30	25	25.7	
30	37	25.5	
30	50	25.2	
30	60	24.8	
40	25		28.5
40	37		28.5
40	50		28.5
40	60		28.5
60	25		27.3
60	37		27.3
60	50		27.3
60	60		27.3
90	25		24.6
90	37		24.6
90	50		24.6
90	60		24.6

Error in lattice parameter measurements is ± 0.1 Å.

Table S2. Lattice parameter of α-Man-OC_8C_4 as a function of water content and temperature.

Water Content (% (w/w))	Temperature (°C)	Lattice parameter (Å)
		L_α
0	25	19.5, 22.6[a]
0	37	19.5, 22.5[a]
0	50	22.4
0	60	22.3
10	25	25.3
10	37	25.2
10	50	24.9
10	60	24.8
20	25	26.6
20	37	26.4
20	50	26.1
20	60	25.9
27.5	25	27.2
27.5	37	27.1
27.5	50	27.1
27.5	60	27.2
40	25	27.1
40	37	27.2
40	50	27.2
40	60	27.4
60	25	27.2
60	37	27.2
60	50	27.4
60	60	27.5
90	25	27.2
90	37	27.2
90	50	27.4
90	60	27.5

Error in lattice parameter measurements is ± 0.1 Å.
[a]Co-existence of two lamellar phases.

Table S3. Lattice parameter of α-Man-$OC_{10}C_6$ as a function of water content and temperature.

Water Content (% (w/w))	Temperature (°C)	Lattice parameter (Å)				
		Metastable	L_α	V_2 (*Ia*3*d*)	V_2 (*Pn*3*m*)	L_2
0	25	?				
0	37		23.8			
0	50		23.7			
0	60					-
7.5	25			68.0		
7.5	37			67.3		
7.5	50			66.6		
7.5	60			66.4		
20	25			79.9		
20	37			78.6		
20	50			77.4		
20	60			76.4		
40	25			81.8	53.8	
40	37			82.4	53.0	
40	50			82.4	52.8	
40	60			81.8	52.6	
70	25			83.5	53.6	
70	37			83.2	53.4	
70	50			83.2	53.2	
70	60			83.4	53.4	
90	25				56.5	
90	37				56.8	
90	50				56.6	
90	60				56.6	

Error in lattice parameter measurements is ± 0.1 Å.

Table S4. Lattice parameter of α-Man-$OC_{12}C_8$ as a function of water content and temperature.

Water Content (% (w/w))	Temperature (°C)	Lattice parameter (Å)			
		V_2 ($Ia3d$)	V_2 ($Pn3m$)	H_2	L_2
0	25	63.0			
0	37	63.0			
0	50				-
0	60				-
7.5	25		42.5	35.0	
7.5	37			34.7	
7.5	50			34.2	
7.5	60			33.6	
20	25			41.4	
20	37			41.3	
20	50			41.0	
20	60			40.7	
40	25			41.4	
40	37			41.1	
40	50			40.8	
40	60			40.7	
70	25			41.0	
70	37			40.7	
70	50			40.5	
70	60			40.2	
90	25			41.9	
90	37			41.8	
90	50			41.5	
90	60			41.4	

Table S5. Lattice parameter of *α*-Man-$OC_{14}C_{10}$ as a function of water content and temperature.

Water Content (% (w/w))	Temperature (°C)	Lattice parameter (Å)
		H_2
0	25	30.0
0	37	29.8
0	50	29.8
0	60	29.8
7.5	25	35.6
7.5	37	35.5
7.5	50	35.1
7.5	60	34.7
15	25	38.9
15	37	38.7
15	50	38.2
15	60	37.5
30	25	42.5
30	37	42.2
30	50	41.9
30	60	41.4
50	25	42.5
50	37	42.2
50	50	41.7
50	60	41.2
70	25	42.3
70	37	41.9
70	50	41.6
70	60	41.3
90	25	42.2
90	37	41.8
90	50	41.4
90	60	41.2

Error in lattice parameter measurements is ± 0.1 Å.

[1]H NMR- 2-ethyl-hexyl-*α*-D-mannopyranoside, *α*-Man-OC_6C_2

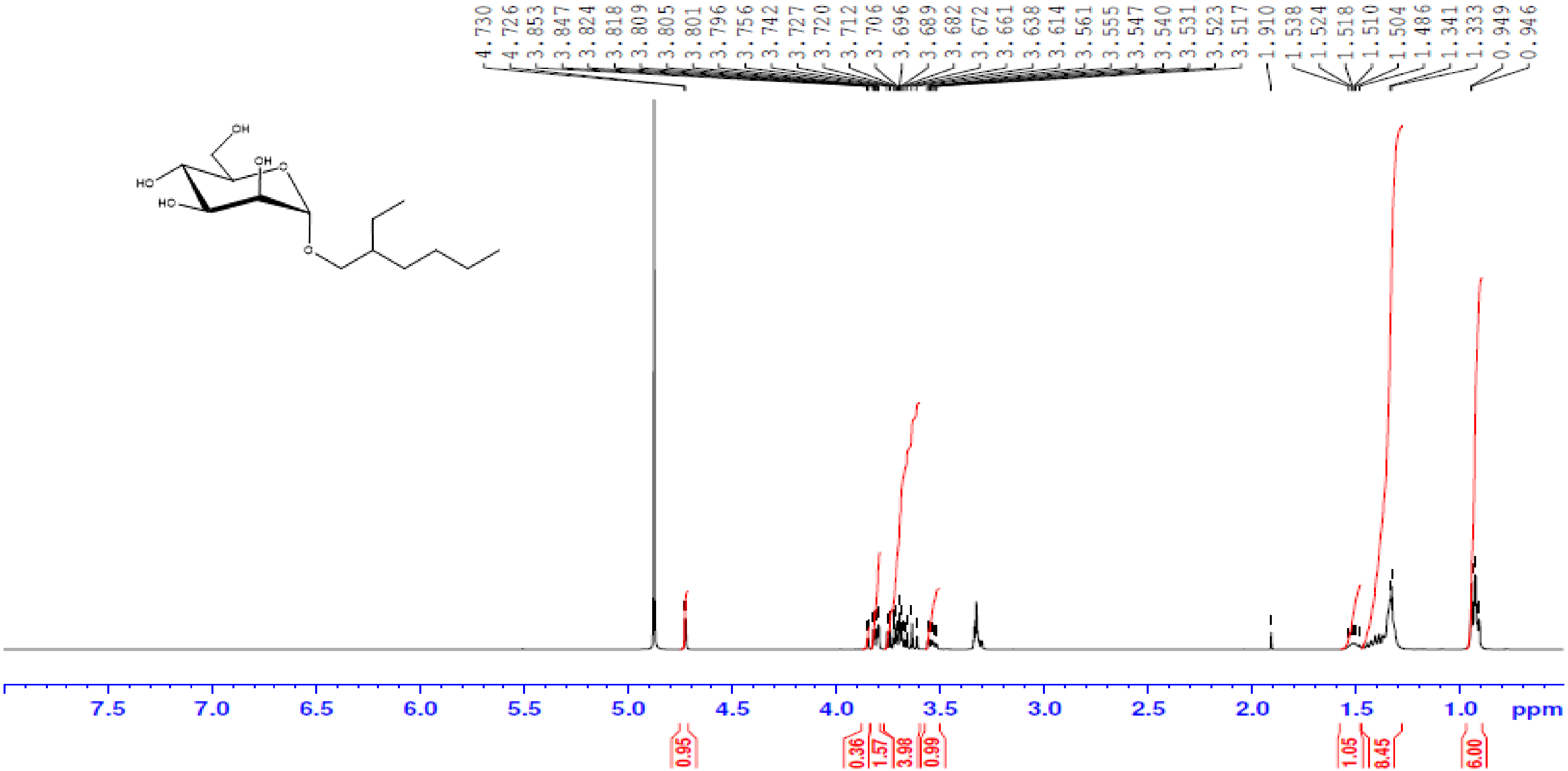

^{13}C NMR- 2-ethyl-hexyl-*α*-D-mannopyranoside, *α*-Man-OC$_6$C$_2$

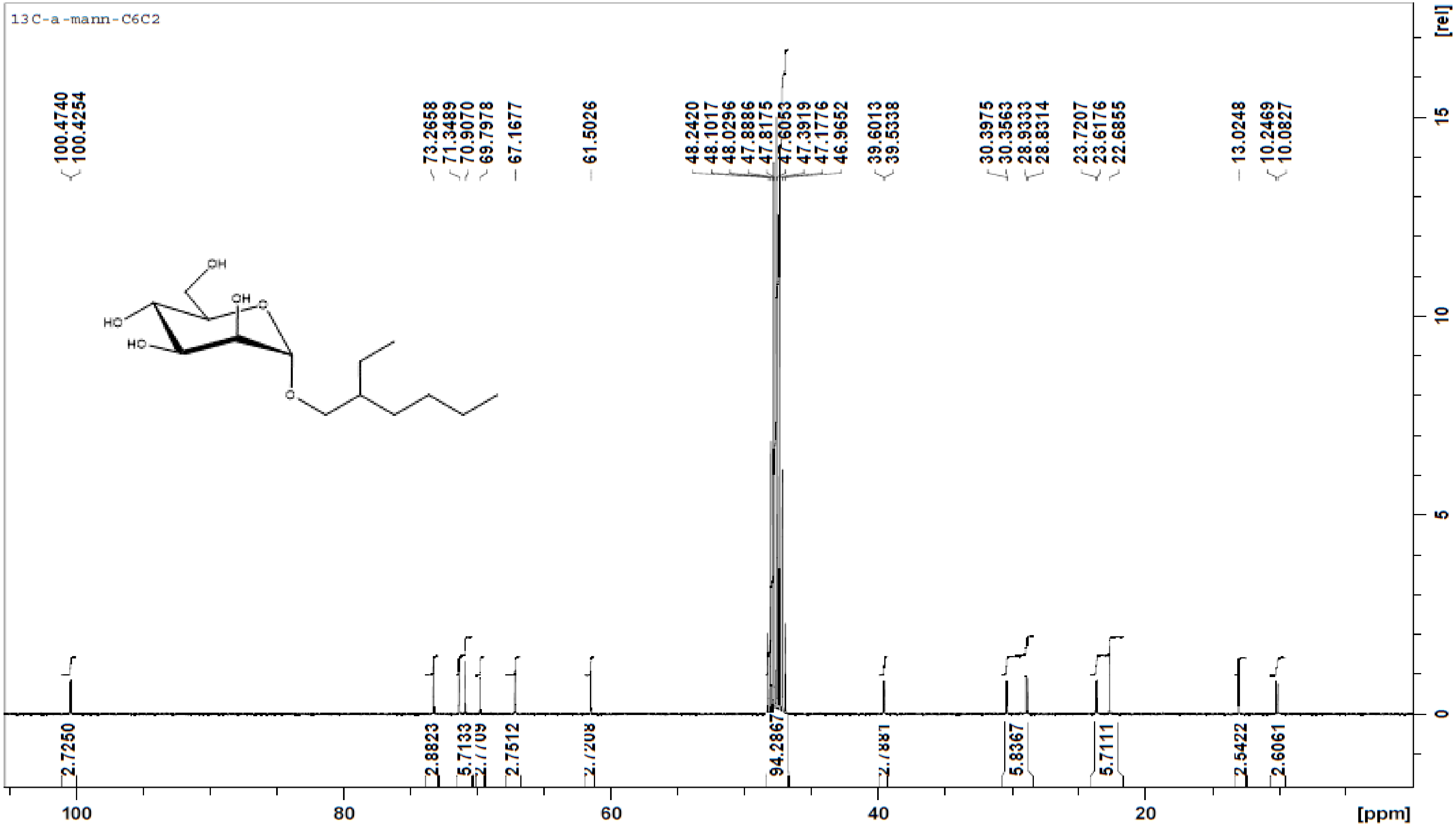

[1]H NMR- 2-butyl-octyl-α-D-mannopyranoside, α-Man-OC8C4

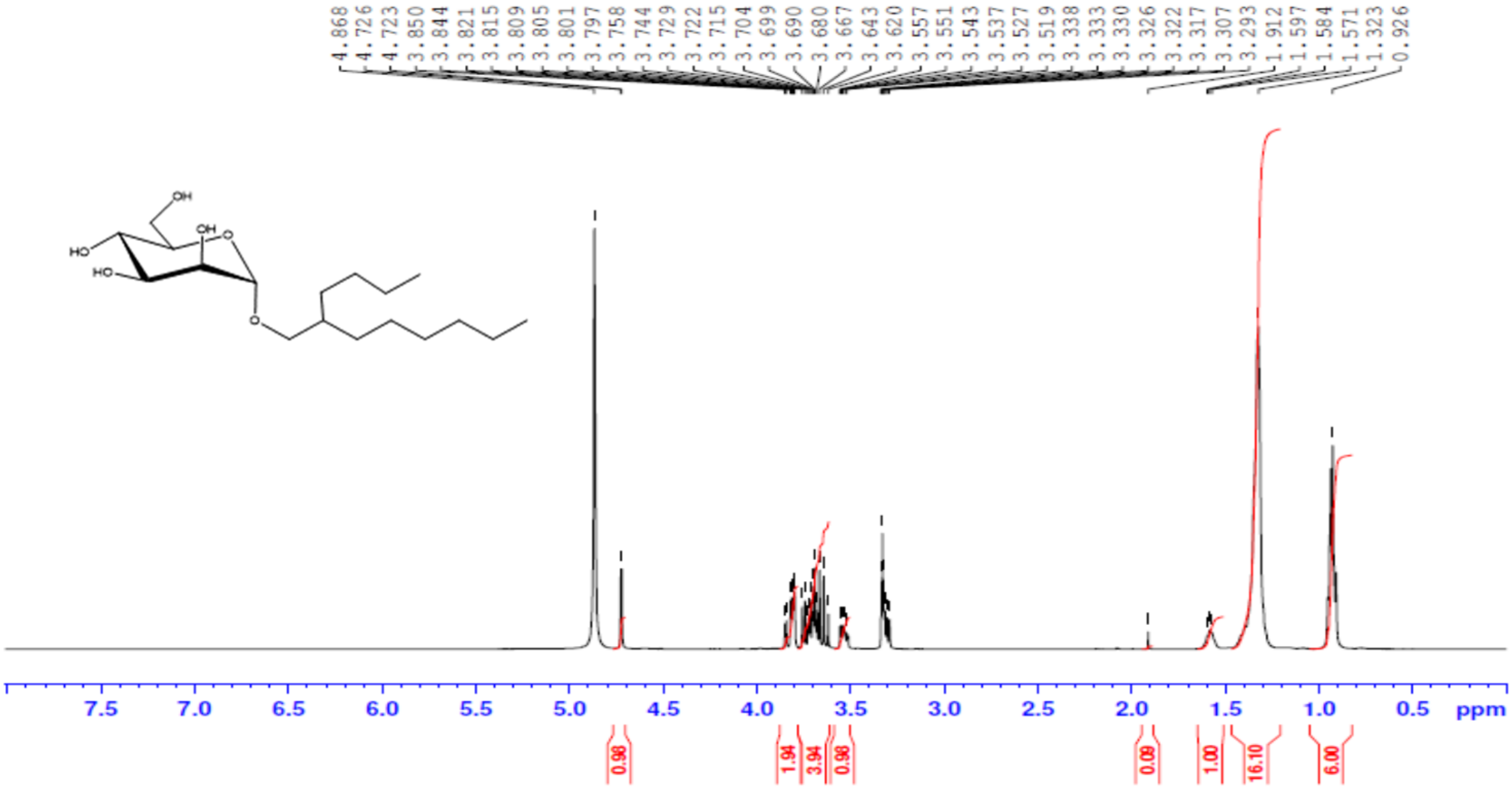

^{13}C NMR- 2-butyl-octyl-*α*-D-mannopyranoside, *α*-Man-OC_8C_4

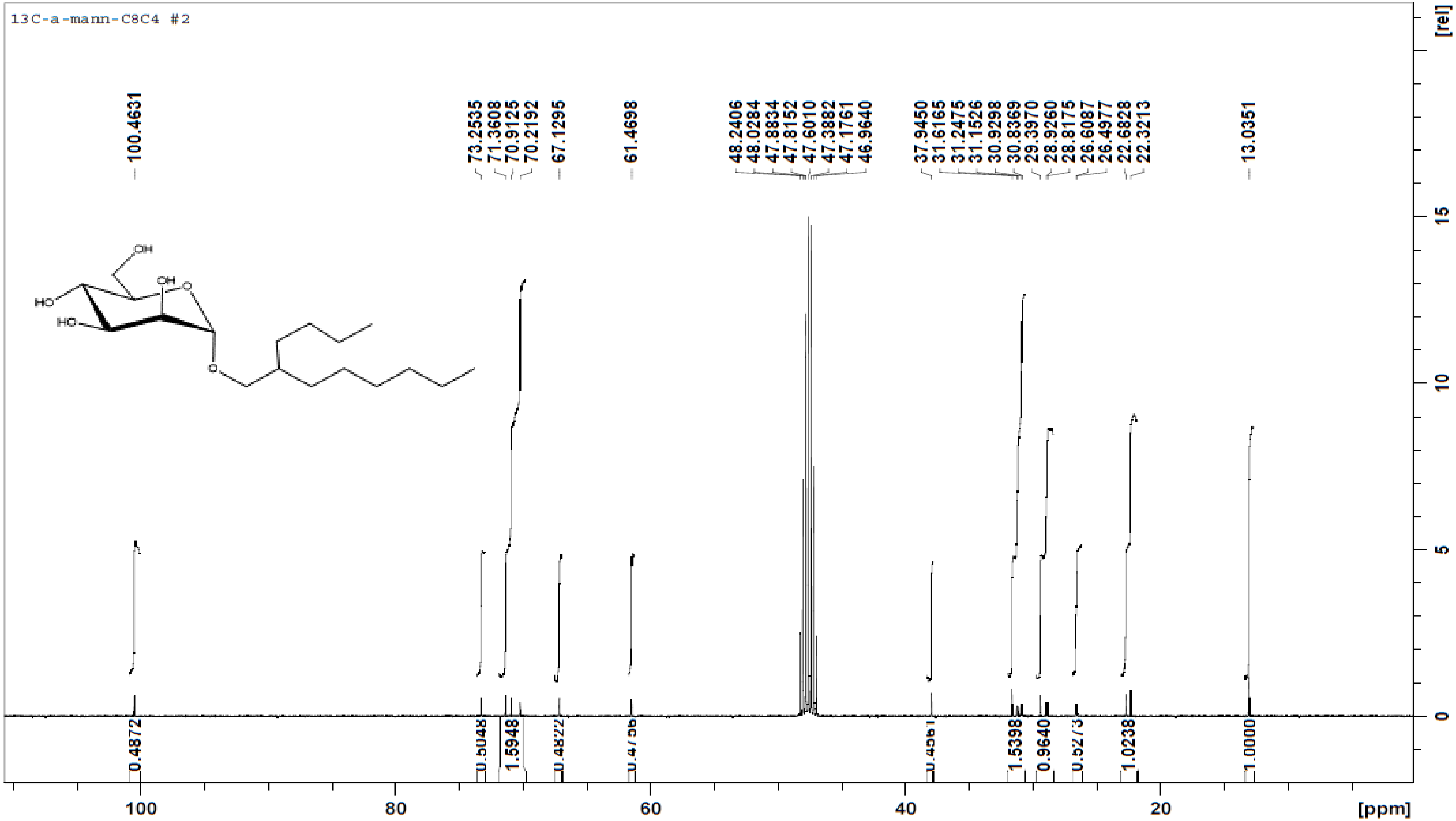

[1]H NMR- 2-hexyl-decyl-α-D-mannopyranoside, α-Man-OC$_{10}$C$_6$

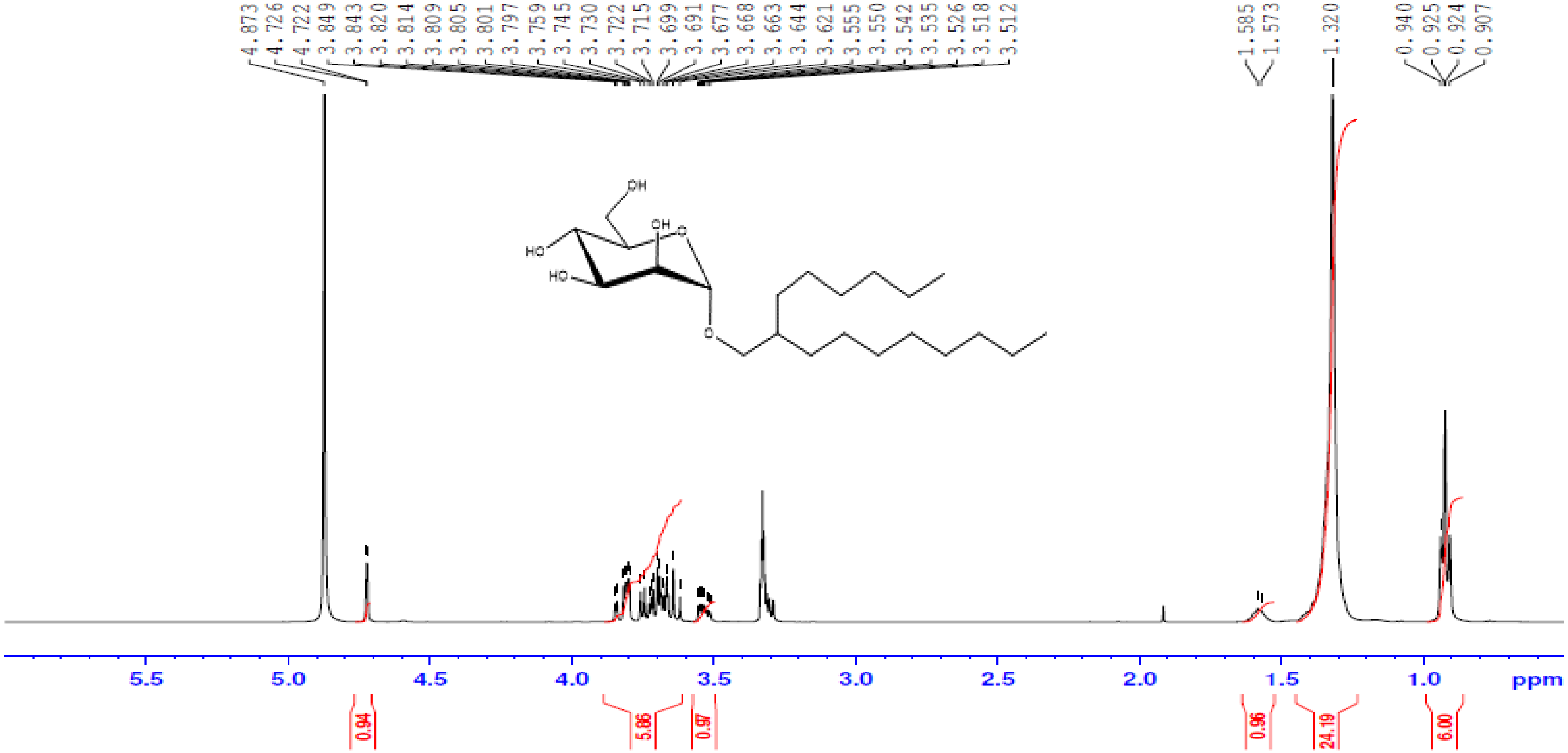

^{13}C NMR- 2-hexyl-decyl-α-D-mannopyranoside, α-Man-OC$_{10}$C$_{6}$

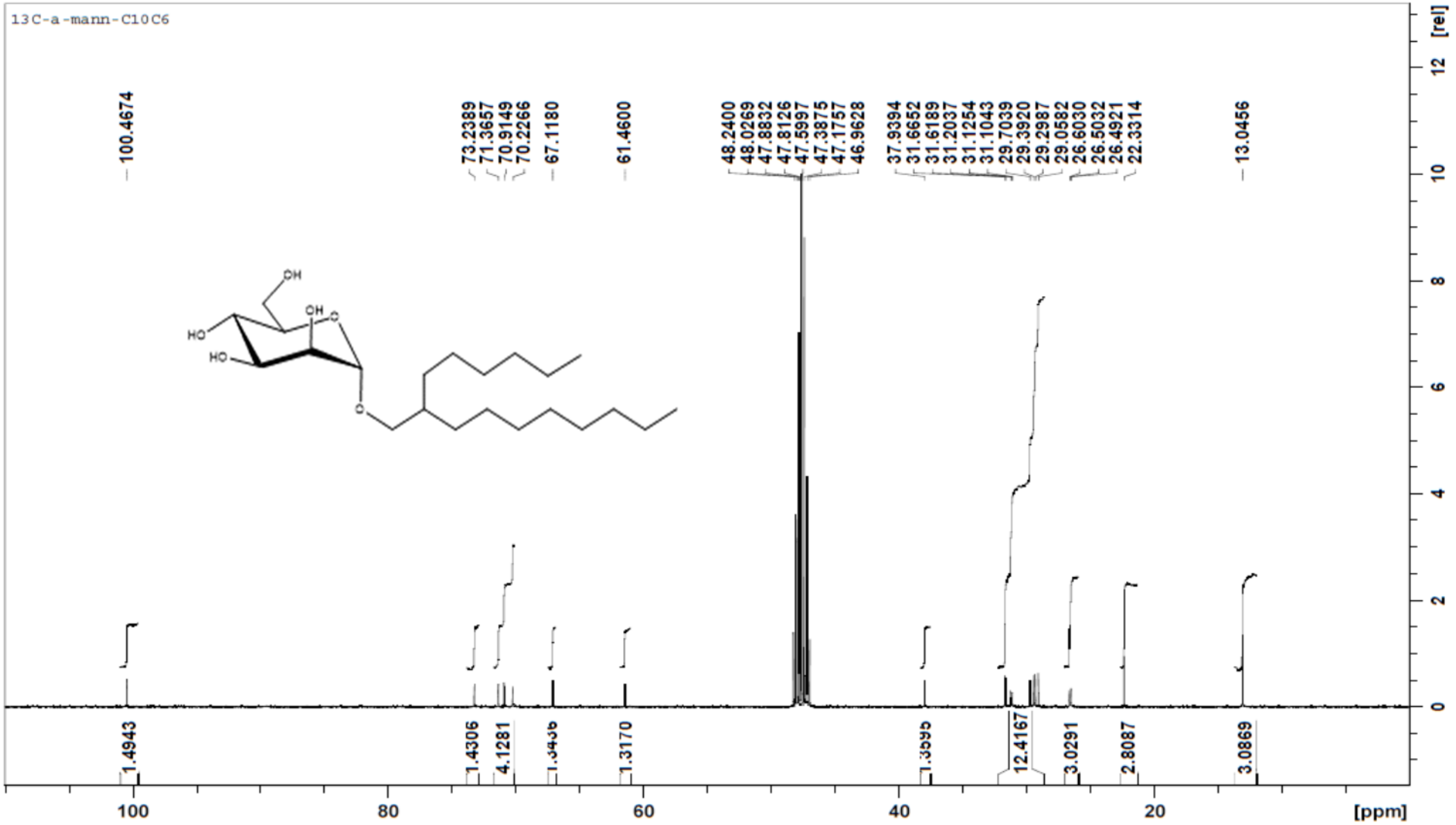

^{1}H NMR- 2-octyl-dodecyl-α-D-mannopyranoside, α-Man-$OC_{12}C_8$

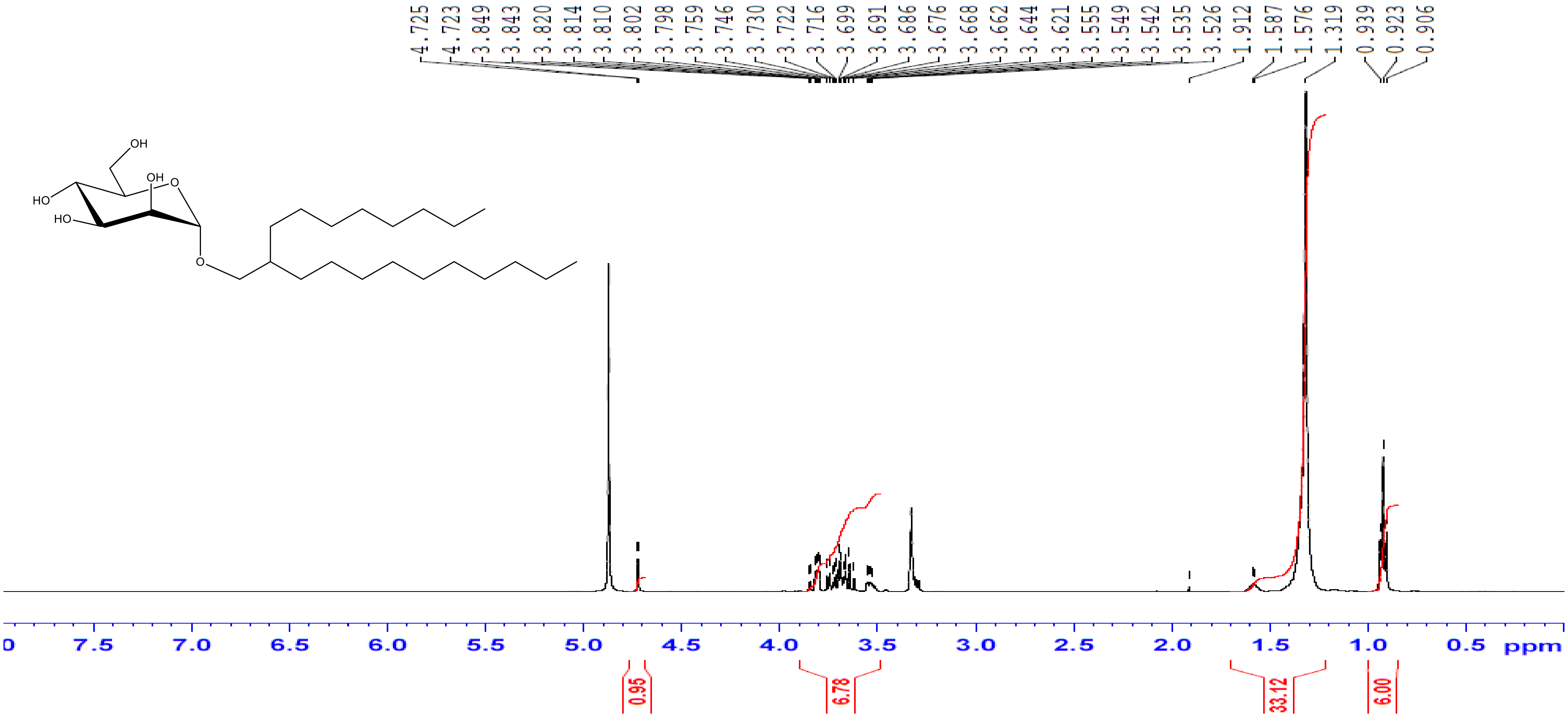

^{13}C NMR- 2-octyl-dodecyl-*α*-D-mannopyranoside, *α*-Man-OC$_{12}$C$_8$

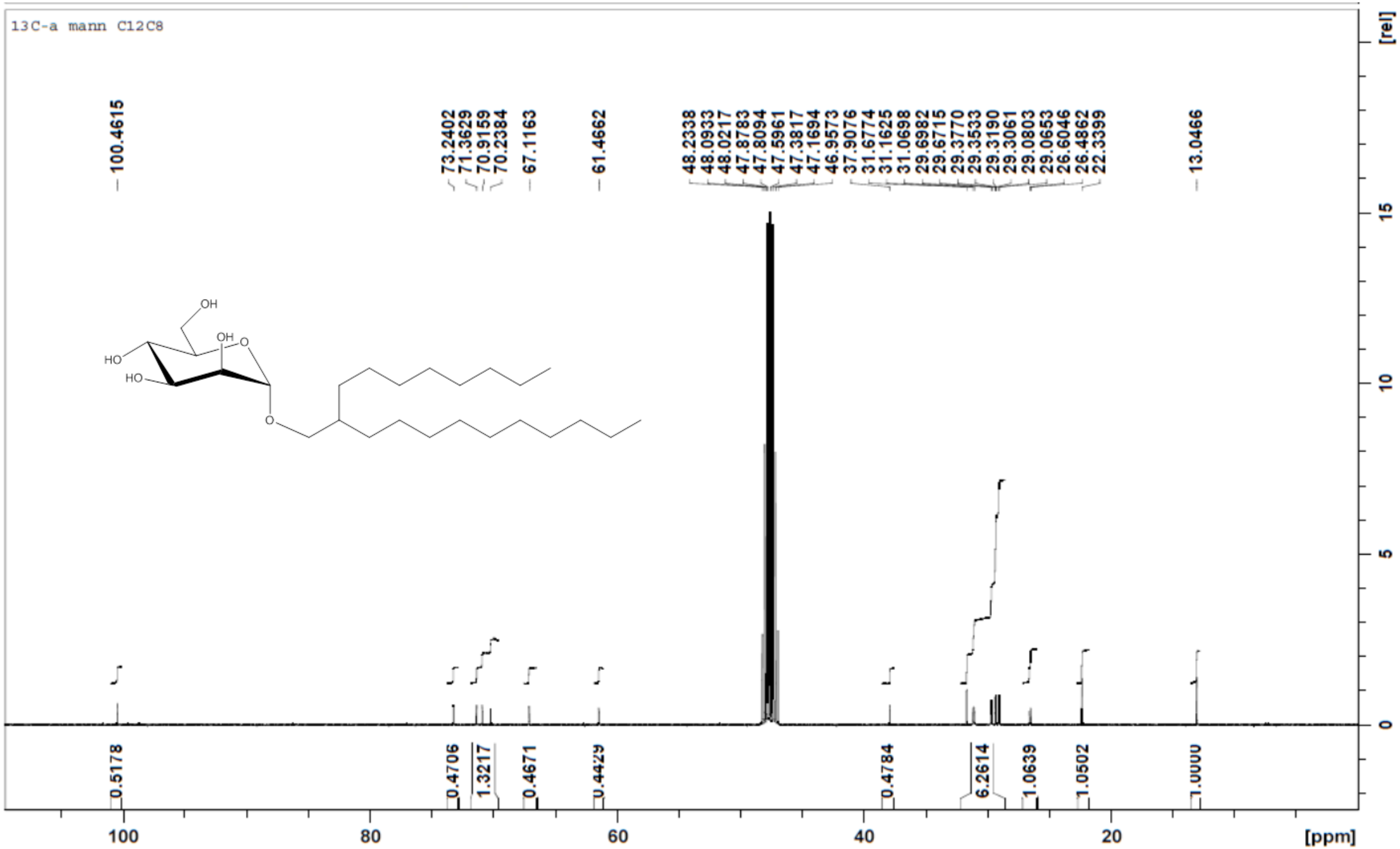

[1]H NMR- 2-decyl-tetradecyl-*α*-D-mannopyranoside, *α*-Man-$OC_{14}C_{10}$

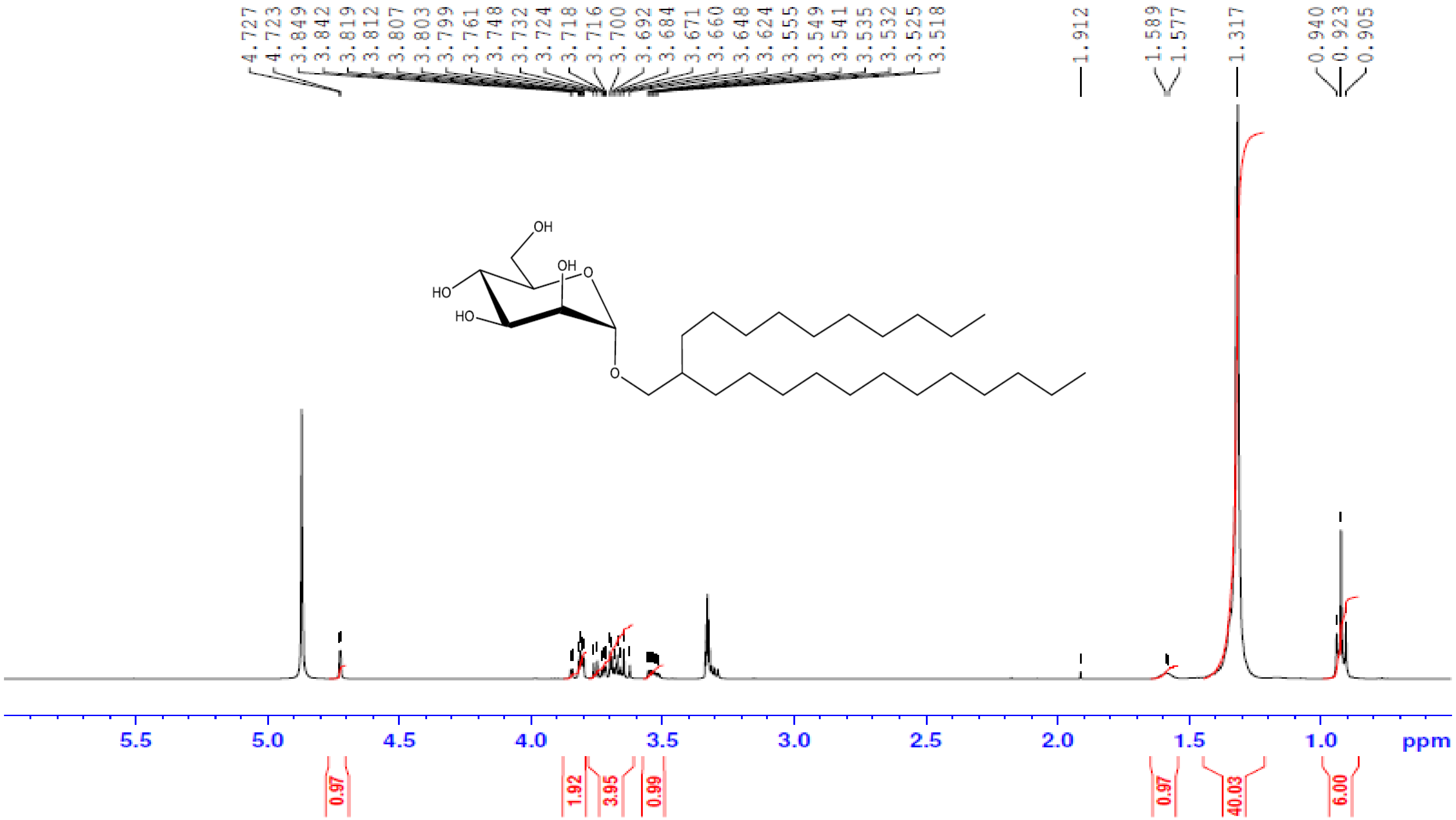

[13]C NMR- 2-decyl-tetradecyl-*α*-D-mannopyranoside, *α*-Man-$OC_{14}C_{10}$